The propagation of a bubble into an elasto-rigid channel

Nico Bergemann

September 20, 2017

0.1 The model

We study the fluid-structure interaction problem of an air bubble propagating into an elasto-rigid channel. The channel width is much larger than the channel depth and therefore we model the fluid flow in the channel by the Hele-Shaw equations. The bottom and side walls of the channel are rigid, whereas the top boundary is formed by an elastic membrane. We expect the transverse displacement of this membrane to be large compared to its thickness and therefore we model its behaviour using the Föppl-von Karman equations.

0.1.1 Fluid equations

We start by deriving the general Hele-Shaw equations in Cartesian coordinates. The incompressible, Cartesian Navier-Stokes equations in three dimensions (x_1, x_2, x_3) are given by

$$\rho\left(\frac{\partial u_1^*}{\partial t^*} + u_1^*\frac{\partial u_1^*}{\partial x_1^*} + u_2^*\frac{\partial u_1^*}{\partial x_2^*} + u_3^*\frac{\partial u_1^*}{\partial x_3^*}\right) = -\frac{\partial p^*}{\partial x_1^*} + \mu\left(\frac{\partial^2 u_1^*}{\partial x_1^{*2}} + \frac{\partial^2 u_1^*}{\partial x_2^{*2}} + \frac{\partial^2 u_1^*}{\partial x_3^{*2}}\right), \tag{1}$$

$$\rho\left(\frac{\partial u_2^*}{\partial t^*} + u_1^*\frac{\partial u_2^*}{\partial x_1^*} + u_2^*\frac{\partial u_2^*}{\partial x_2^*} + u_3^*\frac{\partial u_2^*}{\partial x_3^*}\right) = -\frac{\partial p^*}{\partial x_2^*} + \mu\left(\frac{\partial^2 u_2^*}{\partial x_1^{*2}} + \frac{\partial^2 u_2^*}{\partial x_2^{*2}} + \frac{\partial^2 u_2^*}{\partial x_3^{*2}}\right), \tag{2}$$

$$\rho\left(\frac{\partial u_3^*}{\partial t^*} + u_1^*\frac{\partial u_3^*}{\partial x_1^*} + u_2^*\frac{\partial u_3^*}{\partial x_2^*} + u_3^*\frac{\partial u_3^*}{\partial x_3^*}\right) = -\frac{\partial p^*}{\partial x_3^*} + \mu\left(\frac{\partial^2 u_3^*}{\partial x_1^{*2}} + \frac{\partial^2 u_3^*}{\partial x_2^{*2}} + \frac{\partial^2 u_3^*}{\partial x_3^{*2}}\right), \tag{3}$$

$$\frac{\partial u_1^*}{\partial x_1^*} + \frac{\partial u_2^*}{\partial x_2^*} + \frac{\partial u_3^*}{\partial x_3^*} = 0, \tag{4}$$

where we neglect gravity and any other body forces. We use two different length and velocity scales for non-dimensionalisation, such that

$$(x_1^*, x_2^*) = \mathcal{L}_{x_1x_2}\,(x_1, x_2), \quad x_3^* = \mathcal{L}_{x_3}\,x_3, \quad \text{and} \tag{5}$$

$$(u_1^*, u_2^*) = \mathcal{U}_{u_1u_2}\,(u_1, u_2), \quad u_3^* = \mathcal{U}_{u_3}\,u_3, \tag{6}$$

respectively. With this non-dimensionalisation the continuity equation becomes

$$\frac{\partial u_1}{\partial x_1} + \frac{\partial u_2}{\partial x_2} + \frac{\mathcal{U}_{u_3}\,\mathcal{L}_{x_1x_2}}{\mathcal{U}_{u_1u_2}\,\mathcal{L}_{x_3}}\,\frac{\partial u_3}{\partial x_3} = 0, \tag{7}$$

which is balanced if

$$\frac{\mathcal{U}_{u_3}\,\mathcal{L}_{x_1x_2}}{\mathcal{U}_{u_1u_2}\,\mathcal{L}_{x_3}} = \mathcal{O}(1), \quad \text{or} \quad \mathcal{U}_{u_3} = \frac{\mathcal{L}_{x_3}}{\mathcal{L}_{x_1x_2}}\,\mathcal{U}_{u_1u_2}. \tag{8}$$

We further non-dimensionalise time and pressure on characteristic scales, $t^* = \mathcal{T}\,t$ and $p^* = \mathcal{P}\,p$, respectively, so that the momentum equations become

$$\rho\left(\frac{\mathcal{U}_{u_1u_2}}{\mathcal{T}}\,\frac{\partial u_1}{\partial t}+\frac{\mathcal{U}^2_{u_1u_2}}{\mathcal{L}_{x_1x_2}}\,u_1\frac{\partial u_1}{\partial x_1}+\frac{\mathcal{U}^2_{u_1u_2}}{\mathcal{L}_{x_1x_2}}\,u_2\frac{\partial u_1}{\partial x_2}+\frac{\mathcal{U}^2_{u_1u_2}}{\mathcal{L}_{x_1x_2}}\,u_3\frac{\partial u_1}{\partial x_3}\right)=$$

$$-\frac{\mathcal{P}}{\mathcal{L}_{x_1x_2}}\,\frac{\partial p}{\partial x_1}+\mu\left(\frac{\mathcal{U}_{u_1u_2}}{\mathcal{L}^2_{x_1x_2}}\,\frac{\partial^2 u_1}{\partial x_1^2}+\frac{\mathcal{U}_{u_1u_2}}{\mathcal{L}^2_{x_1x_2}}\,\frac{\partial^2 u_1}{\partial x_2^2}+\frac{\mathcal{U}_{u_1u_2}}{\mathcal{L}^2_{x_3}}\,\frac{\partial^2 u_1}{\partial x_3^2}\right), \tag{9}$$

$$\rho\left(\frac{\mathcal{U}_{u_1u_2}}{\mathcal{T}}\,\frac{\partial u_2}{\partial t}+\frac{\mathcal{U}^2_{u_1u_2}}{\mathcal{L}_{x_1x_2}}\,u_1\frac{\partial u_2}{\partial x_1}+\frac{\mathcal{U}^2_{u_1u_2}}{\mathcal{L}_{x_1x_2}}\,u_2\frac{\partial u_2}{\partial x_2}+\frac{\mathcal{U}^2_{u_1u_2}}{\mathcal{L}_{x_1x_2}}\,u_3\frac{\partial u_2}{\partial x_3}\right)=$$

$$-\frac{\mathcal{P}}{\mathcal{L}_{x_1x_2}}\,\frac{\partial p}{\partial x_2}+\mu\left(\frac{\mathcal{U}_{u_1u_2}}{\mathcal{L}^2_{x_1x_2}}\,\frac{\partial^2 u_2}{\partial x_1^2}+\frac{\mathcal{U}_{u_1u_2}}{\mathcal{L}^2_{x_1x_2}}\,\frac{\partial^2 u_2}{\partial x_2^2}+\frac{\mathcal{U}_{u_1u_2}}{\mathcal{L}^2_{x_3}}\,\frac{\partial^2 u_2}{\partial x_3^2}\right), \tag{10}$$

$$\rho\left(\frac{\mathcal{L}_{x_3}\,\mathcal{U}_{u_1u_2}}{\mathcal{L}_{x_1x_2}\,\mathcal{T}}\,\frac{\partial w}{\partial t}+\frac{\mathcal{U}^2_{u_1u_2}\,\mathcal{L}_{x_3}}{\mathcal{L}^2_{x_1x_2}}\,u_1\frac{\partial u_3}{\partial x_1}+\frac{\mathcal{U}^2_{u_1u_2}\,\mathcal{L}_{x_3}}{\mathcal{L}^2_{x_1x_2}}\,u_2\frac{\partial u_3}{\partial x_2}+\frac{\mathcal{U}^2_{u_1u_2}\,\mathcal{L}_{x_3}}{\mathcal{L}^2_{x_1x_2}}\,u_3\frac{\partial u_3}{\partial x_3}\right)=$$

$$-\frac{\mathcal{P}}{\mathcal{L}_{x_3}}\,\frac{\partial p}{\partial x_3}+\mu\left(\frac{\mathcal{U}_{u_1u_2}\,\mathcal{L}_{x_3}}{\mathcal{L}^3_{x_1x_2}}\,\frac{\partial^2 u_3}{\partial x_1^2}+\frac{\mathcal{U}_{u_1u_2}\,\mathcal{L}_{x_3}}{\mathcal{L}^3_{x_1x_2}}\,\frac{\partial^2 u_3}{\partial x_2^2}+\frac{\mathcal{U}_{u_1u_2}}{\mathcal{L}_{x_1x_2}\,\mathcal{L}_{x_3}}\,\frac{\partial^2 u_3}{\partial x_3^2}\right). \tag{11}$$

We use the intrinsic timescale $\mathcal{T}=\mathcal{L}_{x_1x_2}/\mathcal{U}_{u_1u_2}$, multiply by $\mathcal{L}_{x_1x_2}/(\rho\,\mathcal{U}_{u_1u_2})$ and simplify to yield

$$\frac{\partial u_1}{\partial t}+u_1\frac{\partial u_1}{\partial x_1}+u_2\frac{\partial u_1}{\partial x_2}+u_3\frac{\partial u_1}{\partial x_3}=$$

$$-\frac{\mathcal{P}}{\rho\,\mathcal{U}^2_{u_1u_2}}\,\frac{\partial p}{\partial x_1}+\frac{\mu}{\rho\,\mathcal{U}_{u_1u_2}\,\mathcal{L}_{x_3}}\,\frac{\mathcal{L}_{x_1x_2}}{\mathcal{L}_{x_3}}\,\left[\frac{\mathcal{L}^2_{x_3}}{\mathcal{L}^2_{x_1x_2}}\left(\frac{\partial^2 u_1}{\partial x_1^2}+\frac{\partial^2 u_1}{\partial x_2^2}\right)+\frac{\partial^2 u_1}{\partial x_3^2}\right], \tag{12}$$

$$\frac{\partial u_2}{\partial t}+u_1\frac{\partial u_2}{\partial x_1}+u_2\frac{\partial u_2}{\partial x_2}+u_3\frac{\partial u_2}{\partial x_3}=$$

$$-\frac{\mathcal{P}}{\rho\,\mathcal{U}^2_{u_1u_2}}\,\frac{\partial p}{\partial x_2}+\frac{\mu}{\rho\,\mathcal{U}_{u_1u_2}\,\mathcal{L}_{x_3}}\,\frac{\mathcal{L}_{x_1x_2}}{\mathcal{L}_{x_3}}\,\left[\frac{\mathcal{L}^2_{x_3}}{\mathcal{L}^2_{x_1x_2}}\left(\frac{\partial^2 u_2}{\partial x_1^2}+\frac{\partial^2 u_2}{\partial x_2^2}\right)+\frac{\partial^2 u_2}{\partial x_3^2}\right], \tag{13}$$

$$\frac{\mathcal{L}^2_{x_3}}{\mathcal{L}^2_{x_1x_2}}\left(\frac{\partial u_3}{\partial t}+u_1\frac{\partial u_3}{\partial x_1}+u_2\frac{\partial u_3}{\partial x_2}+u_3\frac{\partial u_3}{\partial x_3}\right)=$$

$$-\frac{\mathcal{P}}{\rho\,\mathcal{U}^2_{u_1u_2}}\,\frac{\partial p}{\partial x_3}+\frac{\mu}{\rho\,\mathcal{U}_{u_1u_2}\,\mathcal{L}_{x_3}}\,\frac{\mathcal{L}_{x_1x_2}}{\mathcal{L}_{x_3}}\,\left[\frac{\mathcal{L}^4_{x_3}}{\mathcal{L}^4_{x_1x_2}}\left(\frac{\partial^2 u_3}{\partial x_1^2}+\frac{\partial^2 u_3}{\partial x_2^2}\right)+\frac{\mathcal{L}^2_{x_3}}{\mathcal{L}^2_{x_1x_2}}\,\frac{\partial^2 u_3}{\partial x_3^2}\right]. \tag{14}$$

We now define the Reynolds number and pressure scale as

$$\mathrm{Re}=\frac{\rho\,\mathcal{U}_{u_1u_2}\,\mathcal{L}_{x_3}}{\mu}\,\frac{\mathcal{L}_{x_3}}{\mathcal{L}_{x_1x_2}},\quad\text{and}\quad\mathcal{P}=\frac{\rho\,\mathcal{U}^2_{u_1u_2}}{\mathrm{Re}}, \tag{15}$$

respectively, so that the non-dimensional, governing momentum equations become

$$\mathrm{Re}\left(\frac{\partial u_1}{\partial t}+u\frac{\partial u_1}{\partial x_1}+v\frac{\partial u_1}{\partial x_2}+u_3\frac{\partial u_1}{\partial x_3}\right)=-\frac{\partial p}{\partial x_1}+\left(\frac{\mathcal{L}_{x_3}}{\mathcal{L}_{x_1x_2}}\right)^2\left(\frac{\partial^2 u_1}{\partial x_1^2}+\frac{\partial^2 u_1}{\partial x_2^2}\right)+\frac{\partial^2 u_1}{\partial x_3^2}, \quad (16)$$

$$\mathrm{Re}\left(\frac{\partial u_2}{\partial t}+u\frac{\partial u_2}{\partial x_1}+u_2\frac{\partial u_2}{\partial x_2}+u_3\frac{\partial u_2}{\partial x_3}\right)=-\frac{\partial p}{\partial x_2}+\left(\frac{\mathcal{L}_{x_3}}{\mathcal{L}_{x_1x_2}}\right)^2\left(\frac{\partial^2 u_2}{\partial x_1^2}+\frac{\partial^2 u_2}{\partial x_2^2}\right)+\frac{\partial^2 u_2}{\partial x_3^2}, \quad (17)$$

$$\left(\frac{\mathcal{L}_{x_3}}{\mathcal{L}_{x_1x_2}}\right)^2\left[\mathrm{Re}\left(\frac{\partial u_3}{\partial t}+u\frac{\partial u_3}{\partial x_1}+u_2\frac{\partial u_3}{\partial x_2}+u_3\frac{\partial u_3}{\partial x_3}\right)-\left(\frac{\mathcal{L}_{x_3}}{\mathcal{L}_{x_1x_2}}\right)^2\left(\frac{\partial^2 u_3}{\partial x_1^2}+\frac{\partial^2 u_3}{\partial x_2^2}\right)-\frac{\partial^2 u_3}{\partial x_3^2}\right]=-\frac{\partial p}{\partial x_3}. \quad (18)$$

We now assume that the height of the channel is much smaller than its width, $\mathcal{L}_{x_3} \ll \mathcal{L}_{x_1x_2}$, so that the aspect ratio $\mathcal{A} = \mathcal{L}_{x_3}/\mathcal{L}_{x_1x_2} \ll 1$, and hence $\mathrm{Re} \ll 1$. With these assumptions the momentum equations simplify to

$$\frac{\partial p}{\partial x_1}=\frac{\partial^2 u_1}{\partial x_3^2}, \quad \frac{\partial p}{\partial x_2}=\frac{\partial^2 u_2}{\partial x_3^2}, \quad \frac{\partial p}{\partial x_3}=0. \quad (19)$$

The resulting velocity field is given by

$$u_1=\frac{1}{2}\frac{\partial p}{\partial x_1}\,x_3^2+Ax_3+B, \quad (20)$$

$$u_2=\frac{1}{2}\frac{\partial p}{\partial x_2}\,x_3^2+Cx_3+D. \quad (21)$$

In order to derive the governing equation, we integrate the continuity equation to get

$$\int_0^b \frac{\partial u_3}{\partial x_3}\,\mathrm{d}x_3=-\int_0^b\left(\frac{\partial u_1}{\partial x_1}+\frac{\partial u_2}{\partial x_2}\right)\mathrm{d}x_3=-\int_0^b\frac{\partial u_1}{\partial x_1}\,\mathrm{d}x_3-\int_0^b\frac{\partial u_2}{\partial x_2}\,\mathrm{d}x_3. \quad (22)$$

Using the Leibniz Theorem we obtain

$$[u_3]_0^b=-\frac{\partial}{\partial x_1}\left(\int_0^b u_1\,\mathrm{d}x_3\right)-\frac{\partial}{\partial x_2}\left(\int_0^b u_2\,\mathrm{d}x_3\right). \quad (23)$$

0.1.2 Membrane equations

We model the elastic sheet on top of the channel using the Föppl-von Karman equations in terms of in-plane displacements v_i^* which are given by (Landau and Lifshitz, 1959)

$$\frac{E\,h^3}{12(1-\nu^2)}\,\nabla^{*4}w^*-h\frac{\partial}{\partial x_j^*}\left(\sigma_{ij}^*\frac{\partial w^*}{\partial x_i^*}\right)=P^* \quad (24)$$

$$\frac{\partial \sigma_{ij}^*}{\partial x_j^*}=t_i^*, \quad (25)$$

where E, ν and h are the Young's modulus, Poisson's ratio and thickness of the membrane, respectively, and P^* and t_i^* are the pressure and in-plane traction excerted onto the sheet, respectively. The unknowns are the two components v_1^* and v_2^* of the displacement vector $\boldsymbol{v}^*$ and the transverse displacement w^*. The components of the stress tensor are given by

$$\sigma_{11}^* = \sigma_{11}^{(0)*} + \frac{E}{1-\nu^2}\left(\epsilon_{11} + \nu\,\epsilon_{22}\right), \tag{26}$$

$$\sigma_{22}^* = \sigma_{22}^{(0)*} + \frac{E}{1-\nu^2}\left(\epsilon_{22} + \nu\,\epsilon_{11}\right), \tag{27}$$

$$\sigma_{12}^* = \sigma_{21}^* = \sigma_{12}^{(0)*} + \frac{E}{1+\nu}\,\epsilon_{12}, \tag{28}$$

where $\boldsymbol{\epsilon}$ is the strain tensor and $\boldsymbol{\sigma}^{(0)*}$ is the pre-stress tensor. We non-dimensionalise the equations on the in-plane length scale $\mathcal{L}_{x_1x_2}$ and the Young's modulus E such that

$$\begin{aligned} (x_i^*, v_i^*, w^*) = \mathcal{L}_{x_1x_2}\,(x_i, v_i, w), \quad \nabla^* = \frac{1}{\mathcal{L}_{x_1x_2}}\,\nabla, \\ \sigma_{ij}^* = E\,\sigma_{ij}, \quad t_i^* = E\mathcal{L}_{x_1x_2}\,t_i, \quad P^* = \frac{K}{\mathcal{L}_{x_1x_2}^3}\,P, \end{aligned} \tag{29}$$

and define the following parameters

$$K = \frac{E\,h^3}{12(1-\nu^2)}, \qquad \eta = 12(1-\nu^2)\left(\frac{\mathcal{L}_{x_1x_2}}{h}\right)^2. \tag{30}$$

The non-dimensional equations then become

$$\nabla^4 w - \eta\frac{\partial}{\partial x_j}\left(\sigma_{ij}\frac{\partial w}{\partial x_i}\right) = P \tag{31}$$

$$\frac{\partial \sigma_{ij}}{\partial x_j} = t_i, \tag{32}$$

with the components of the stress tensor given by

$$\sigma_{11} = \sigma_{11}^{(0)} + \frac{1}{1-\nu^2}\left(\epsilon_{11} + \nu\,\epsilon_{22}\right), \tag{33}$$

$$\sigma_{22} = \sigma_{22}^{(0)} + \frac{1}{1-\nu^2}\left(\epsilon_{22} + \nu\,\epsilon_{11}\right), \tag{34}$$

$$\sigma_{12} = \sigma_{21} = \sigma_{12}^{(0)} + \frac{1}{1+\nu}\,\epsilon_{12}. \tag{35}$$

0.1.3 The coupled problem

The fluid and membrane equations are coupled through the pressure term in the Föppl-von Karman equations, which depends on the pressure in the fluid and the bubble:

$$P = \begin{cases} \mathcal{I}\, p_B & \text{in } \Omega_{\text{air}}, \\ \mathcal{I}\, p & \text{in } \Omega_{\text{fluid}}, \end{cases} \tag{36}$$

where the non-dimensional interaction parameter, $\mathcal{I}$, is a measure of the typical viscous stresses in the fluid relative to the stiffness of the elastic membrane. In particular, for $\mathcal{I} \to 0$ we recover the behaviour of a rigid-walled Hele-Shaw cell. Moreover, the transverse deflection of the membrane affects the depth of the Hele-Shaw cell

$$b = 1 + w/\mathcal{A}. \tag{37}$$

Note that we neglect the coupling through in-plane shear stresses.

0.2 Lab frame

0.2.1 Governing equation

In the lab frame, we apply the no-slip ($\boldsymbol{u} \cdot \boldsymbol{t} = 0$) and no penetration ($\boldsymbol{u} \cdot \boldsymbol{n} = 0$) boundary conditions at the top and bottom walls, $x_3 = b(x_1, x_2)$ and $x_3 = 0$, respectively. With these boundary conditions the velocity field becomes

$$u_1 = \frac{1}{2}\frac{\partial p}{\partial x_1}(x_3^2 - b x_3), \tag{38}$$

$$u_2 = \frac{1}{2}\frac{\partial p}{\partial x_2}(x_3^2 - b x_3), \tag{39}$$

and $u_3(x_3 = 0) = 0$ at the rigid bottom wall, and $u_3(x_3 = b) = \partial b/\partial t$ at the elastic top wall. The governing equation then becomes

$$\frac{\partial b}{\partial t} = -\frac{\partial}{\partial x_1}\left[-\frac{1}{12}b^3\frac{\partial p}{\partial x_1}\right] - \frac{\partial}{\partial x_2}\left[-\frac{1}{12}b^3\frac{\partial p}{\partial x_2}\right], \tag{40}$$

or employing the summation convention with $i = \{1, 2\}$,

$$\frac{\partial b}{\partial t} = \frac{\partial}{\partial x_i}\left[\frac{1}{12}b^3\frac{\partial p}{\partial x_i}\right]. \tag{41}$$

The flux in the x_1-direction at any given point is given by

$$q_{x_1} = \int_0^b u_1 \mathrm{d}x_3 = \bar{u}_1 b, \tag{42}$$

where $\bar{u}_1$ is the depth-averaged velocity in the x_1-direction, which is defined as

$$\bar{u}_1 = \frac{1}{b}\int_0^b u_1 \,\mathrm{d}x_3 = -\frac{1}{12}b^2\frac{\partial p}{\partial x_1}, \tag{43}$$

and similarly

$$\bar{u}_2 = -\frac{1}{12} b^2 \frac{\partial p}{\partial x_2}. \tag{44}$$

We choose to re-define the pressure scale as

$$\mathcal{P} = \frac{12 \rho \mathcal{U}_{u_1 u_2}^2}{\mathrm{Re}}, \tag{45}$$

so that the governing equation becomes

$$\frac{\partial b}{\partial t} = \frac{\partial}{\partial x_i} \left(b^3 \frac{\partial p}{\partial x_i} \right). \tag{46}$$

with the depth-averaged velocities

$$\bar{u}_1 = -b^2 \frac{\partial p}{\partial x_1}, \quad \text{and} \quad \bar{u}_2 = -b^2 \frac{\partial p}{\partial x_2}. \tag{47}$$

0.2.2 Kinematic and dynamic boundary conditions

At the air-liquid interface, whose position we describe by $R_i = R_i^* / W_{\text{channel}} = R_i(S, t)$, we apply the kinematic boundary condition

$$\frac{\partial R_i}{\partial t} \, n_i = \bar{u}_i \, n_i = -b^2 \frac{\partial p}{\partial x_i} \, n_i \quad \text{at } \partial \Omega_{\text{air}}, \tag{48}$$

where n_i is the unit normal at the interface pointing into the viscous fluid. The dynamic boundary condition arising from the capillary pressure jump across the interface is given by

$$p|_{\partial \Omega_{\text{air}}} = p_B - \frac{1}{12} Ca^{-1} \, \mathcal{A} \, \kappa_{\text{mean}}, \tag{49}$$

where $Ca = \mu W_{\text{channel}} / (\gamma \mathcal{T})$ is the capillary number. The non-dimensional mean curvature of the interface, $\kappa_{\text{mean}} = W_{\text{channel}} \, \kappa_{\text{mean}}^*$, is approximated by the sum of in-plane and transverse curvatures as

$$\kappa_{\text{mean}} = \mathcal{A} \, \frac{\partial m_i}{\partial S} \, n_i + \frac{2}{b}, \tag{50}$$

where m_i is the in-plane unit tangent to the interface, pointing in the direction of increasing arclength $S = S^* / W_{\text{channel}}$. The term $2/b$ is an approximation of the transverse curvature. We also note that in the dynamic boundary condition we neglect viscous normal stresses at the interface. So far we neglected any thin liquid films between the propagating air bubble and the bounding walls of the Hele-Shaw channel, which may be present in the physical system. However, we are able to incorporate thin film effects in the depth-averaged Hele-Shaw formulation by modifying the kinematic and dynamic boundary conditions at the air-liquid interface as proposed by Peng et al. (2015). Hence, the modified kinematic boundary condition becomes

$$(1 - f_1(Ca)) \, \frac{\partial R_i}{\partial t} \, n_i + f_1(Ca) \bar{u}_i^{\text{film}} \, n_i = \bar{u}_i \, n_i \text{at } \partial \Omega_{\text{air}}, \tag{51}$$

where the fluid velocities in the film are given by (Reinelt and Saffman, 1985)

$$\bar{u}_i^{\text{film}} = -f_1^2(Ca)b^2 \frac{\partial p}{\partial x_i}, \tag{52}$$

where the pressure gradient is the one in the thin films. We do not compute the pressure distribution in the films and therefore approximate it by the pressure gradient in the bulk at the point of the interface. The dynamic boundary condition becomes

$$p - p_b + \frac{\alpha}{12Ca}\left(\alpha \frac{\partial m_i}{\partial S} \cdot n_i + \frac{2f_2(Ca)}{b}\right) = 0. \tag{53}$$

The functions $f_1(Ca)$ and $f_2(Ca)$ are given by (Peng et al., 2015)

$$f_1(Ca) = \frac{Ca^{2/3}}{0.76 + 2.16Ca^{2/3}}, \qquad f_2(Ca) = 1 + \frac{Ca^{2/3}}{0.26 + 1.48Ca^{2/3}} + 1.59Ca. \tag{54}$$

In the limit of $Ca \to \infty$, f_1 tends to a constant value, while f_2 becomes proportional to Ca. With this proportionality, examination of the dynamic boundary condition indicates that the transverse curvature $2/b$ becomes the dominant term as $Ca \to \infty$, whereas the in-plane curvature is insignificant. The total thickness of the liquid films at the top and bottom of the bubble is $h_{\text{film}} = f_1(Ca)b$. We note that according to Peng et al. (2015) the Capillary number used when evaluating f_1 and f_2 should be the local Capillary number at the interface, $Ca_{\text{local}} = Ca\, u_{\text{interface}}$, where $u_{\text{interface}} = (u_1^2 + u_2^2)^{1/2}$. This, however, results in a varying film thickness along the bubble, which has to be taken into consideration when calculating the bubble volume enclosed in the channel. We found that this is numerically unstable and therefore use the "global" Capillary number, Ca, when evaluating the functions.

0.2.3 Problem setup

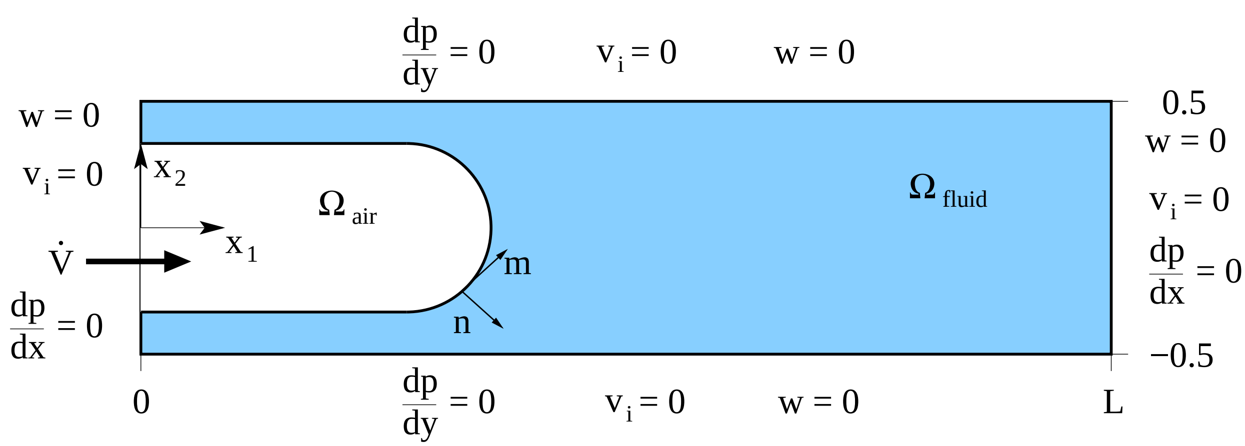

Figure 1: A schematic diagram of a long, finite-sized bubble propagating into an elasto-rigid channel. Boundary conditions as shown, where p is the fluid pressure, w the transverse displacement of the elastic sheet, and v_i the in-plane displacements of the sheet.

A schematic diagram of the specific problem setup is shown in figure 1: a rectangular Hele-Shaw channel with an elastic membrane as upper boundary. In the undeformed configuration the channel has a uniform depth, b_0, which sets the length scale in the transverse direction of the channel, $\mathcal{L}_{x_3} = b_0$. We choose the channel width as the in-plane length scale $\mathcal{L}_{x_1 x_2} = W_{\text{channel}}$ and $b_0 \ll W_{\text{channel}}$ holds. Air is injected at a constant volume flow rate, $\dot{V}$, into the bubble, occupying the region Ω_{air}, which displaces a viscous fluid (of viscosity μ and surface tension γ) which occupies the region Ω_{fluid}. The bubble volume at any time, t, is given by $V = V_{\text{initial}} + t$, where V_{initial} is the initial bubble volume. We base the characteristic velocity scale on the constant volume flow rate, such that $\mathcal{U}_{u_1 u_2} = \dot{V}/(W_{\text{channel}}\, b_0)$. The characteristic (instrinsic) time scale is given by $\mathcal{T} = W_{\text{channel}}^2\, b_0/\dot{V}$. The fluid pressure scale becomes $\mathcal{P} = 12\dot{V}\mu/b_0^3$. On the channel side walls we impose zero transverse ($w = 0$) and in-plane displacements ($v_i = 0$), corresponding to clamped boundaries. Far ahead and far behind the bubble tip we impose zero in-plane displacements ($v_i = 0$), while we leave the transverse displacement undetermined, and instead impose zero slope, $\partial w/\partial x_1 = 0$. The interaction parameter is given by $\mathcal{I} = 12\dot{V}\mu/(\mathcal{A}^3 K)$.

0.3 Moving frame

We are now seeking solutions in a frame of reference moving at the velocity of the air bubble, U_B, so that we perform the following coordinate transformations

$$X_1 = x_1 - U_B\, t, \quad X_2 = x_2, \quad X_3 = x_3, \quad T = t, \tag{55}$$

and the velocity transformations

$$U_1 = u_1 - U_B, \quad U_2 = u_2, \quad U_3 = u_3. \tag{56}$$

This translates into the following derivatives in the moving frame

$$\frac{\partial}{\partial x_1} = \frac{\partial}{\partial X_1}, \quad \frac{\partial}{\partial x_2} = \frac{\partial}{\partial X_2}, \quad \frac{\partial}{\partial x_3} = \frac{\partial}{\partial X_3}, \quad \frac{\partial}{\partial t} = -U_B \frac{\partial}{\partial X_1} + \frac{\partial}{\partial T}. \tag{57}$$

Here, $U_B\, t = x_{\text{tip}}$ describes the bubble tip location for a constant U_B. For a bubble tip velocity which is varying in time, the temporal history is required to define the tip location, $x_{\text{tip}} = \int U_B(t)\, t\, \mathrm{d}t$ and the temporal derivative has to include a frame acceleration term. However, we operate in a Stokes regime, $Re \ll 1$, so that history and frame acceleration can be neglected. This means that in our case U_B is the instantaneous bubble tip velocity, which can be varying in time. The velocity field in the moving frame is then given by

$$U_1 + U_B = \frac{1}{2}\frac{\partial p}{\partial X_1} X_3^2 + A X_3 + B, \tag{58}$$

$$U_2 = \frac{1}{2}\frac{\partial p}{\partial X_2} X_3^2 + C X_3 + D. \tag{59}$$

We apply the no-slip ($U_1 = -U_B$) and no penetration ($U_2 = 0$) boundary conditions at the top and bottom walls, $x_3 = b(x_1, x_2)$ and $x_3 = 0$, respectively. With these boundary conditions the velocity field becomes

$$U_1 = \frac{1}{2}\frac{\partial p}{\partial X_1}(X_3^2 - bX_3) - U_B, \tag{60}$$

$$U_2 = \frac{1}{2}\frac{\partial p}{\partial X_2}(X_3^2 - bX_3). \tag{61}$$

and $U_3(X_3 = 0) = 0$ at the rigid bottom wall, and $U_3(X_3 = b) = -U_B \partial b/\partial X_1 + \partial b/\partial T$ at the elastic top wall. The governing equation then becomes

$$-U_B\frac{\partial b}{\partial X_1} + \frac{\partial b}{\partial T} = -\frac{\partial}{\partial X_1}\left[-\frac{1}{12}b^3\frac{\partial p}{\partial X_1}\right] - \frac{\partial}{\partial X_2}\left[-\frac{1}{12}b^3\frac{\partial p}{\partial X_2}\right], \tag{62}$$

or employing the summation convention with $i = \{1, 2\}$,

$$-U_{B,i}\frac{\partial b}{\partial X_i} + \frac{\partial b}{\partial T} = \frac{\partial}{\partial X_i}\left[\frac{1}{12}b^3\frac{\partial p}{\partial X_i}\right], \tag{63}$$

where $U_{B,2} = 0$ in our case. The flux in the X_1-direction at any given point is given by

$$q_{X_1} = \int_0^b U_1 \mathrm{d}X_3 = \bar{U}_1 b, \tag{64}$$

where $\bar{U}_1$ is the depth-averaged velocity in the X_1-direction, which is defined as

$$\bar{U}_1 = \frac{1}{b}\int_0^b U_1 \, \mathrm{d}X_3 = -\frac{1}{12}b^2\frac{\partial p}{\partial X_1} - U_B, \tag{65}$$

and similarly

$$\bar{U}_2 = -\frac{1}{12}b^2\frac{\partial p}{\partial X_2}. \tag{66}$$

We choose to re-define the pressure scale as

$$\mathcal{P} = \frac{12\rho\mathcal{U}_{u_1u_2}^2}{\mathrm{Re}}, \tag{67}$$

so that the governing equation becomes

$$-U_{B,i}\frac{\partial b}{\partial X_i} + \frac{\partial b}{\partial T} = \frac{\partial}{\partial X_i}\left(b^3\frac{\partial p}{\partial X_i}\right). \tag{68}$$

with the depth-averaged velocities

$$\bar{U}_1 = -b^2\frac{\partial p}{\partial X_1} - U_B, \quad \text{and} \quad \bar{U}_2 = -b^2\frac{\partial p}{\partial X_2}. \tag{69}$$

We note that for $U_B = 0$ we recover the equations derived in the lab frame.

0.3.1 Kinematic and dynamic boundary conditions

The kinematic boundary condition in the moving frame is given by

$$\frac{\partial R_i}{\partial T}\, n_i = \bar{U}_i\, n_i = -b^2 \frac{\partial p}{\partial X_i}\, n_i - U_{B,i}\, n_i \quad \text{at } \partial\Omega_{\text{air}}, \tag{70}$$

where n_i is the unit normal at the interface pointing into the viscous fluid. The dynamic boundary condition is independent of the frame of reference and hence remains unchanged. Again we can modify the kinematic boundary condition to incorporate thin film effects, so that it becomes

$$(1 - f_1(Ca))\, \frac{\partial R_i}{\partial t}\, n_i + f_1(Ca)\bar{U}_i^{\text{film}}\, n_i = \bar{U}_i\, n_i \text{at } \partial\Omega_{\text{air}}. \tag{71}$$

The fluid velocity in the thin films is given by

$$\bar{U}_i^{\text{film}} = -f_1^2(Ca) b^2 \frac{\partial p}{\partial X_i} - U_{B,i}. \tag{72}$$

Here, $\partial p/\partial X_i$ is the pressure gradient in the thin films, at the air-liquid interface, i.e. the transition region from the fluid bulk to the films. We take this gradient to be the same gradient as the one in the bulk at this location. The mass flow into the thin films is

$$\int_{\partial\Omega_{\text{air}}} f_1(Ca) b\, \bar{u}_i^{\text{film}}\, n_i \,\mathrm{d}S, \tag{73}$$

Similarly to the argument employed in the lab frame, we base the evaluation of f_1 (and f_2) on the "global" Capillary number, because using a locally defined one would result in spatially varying film thicknesses and associated numerical instabilities.

0.3.2 Problem setup – full, fixed U_B

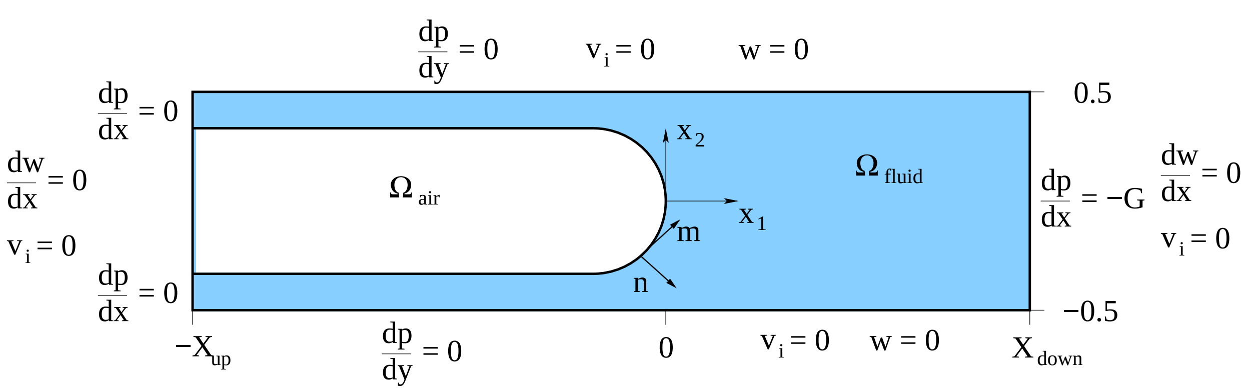

Figure 2: A schematic diagram of a semi-infinite bubble propagating into an elasto-rigid channel. Boundary conditions as shown, where p is the fluid pressure, w the transverse displacement of the elastic sheet, and v_i the in-plane displacements of the sheet.

A schematic diagram of the specific problem setup is shown in Fig. 2: a rectangular Hele-Shaw channel with an elastic membrane as upper boundary. In the undeformed configuration the channel has a uniform depth, b_0, which sets the length scale in the transverse direction of the channel, $\mathcal{L}_{x_3} = b_0$. We choose the channel width as the in-plane length scale $\mathcal{L}_{x_1x_2} = W_{\text{channel}}$ and $b_0 \ll W_{\text{channel}}$ holds. A propagating semi-infinite air bubble, occupying the region Ω_{air} and moving with U_B^* displaces a viscous fluid (of viscosity μ and surface tension γ) which occupies the region Ω_{fluid}. We choose the propagation speed of the bubble as characteristic velocity scale, $\mathcal{U}_{u_1u_2} = U_B^*$. The streamwise position of the tip of the air bubble is held at a prescribed position, $x_{\text{prescribed}} = 0$, which is used as a constraint to determine the unknown pressure in the air bubble, $p_B = p_B^*/\mathcal{P}$, with $\mathcal{P} = 12\mu U_B^*/(b_0\mathcal{A})$. Far ahead of the bubble we apply the streamwise pressure gradient $\partial p/\partial X_1 = -G$, which is unknown *a priori* and is determined as part of the solution such that the flux ahead of the bubble corresponds to the prescribed value, Q_∞. Far behind the bubble we assume the fluid is at rest, $\partial p/\partial X_1 = 0$. On the side walls of the channel we impose non-permeability, $\partial p/\partial X_2 = 0$. At the upstream end of the domain, we prescribe the bubble interface to be parallel to the top and bottom walls by setting the X_2-component of the tangent vectors at these two points to zero. On the channel top and bottom walls we impose zero transverse and in-plane displacements, corresponding to clamped boundaries. Far ahead and far behind the bubble tip we impose zero normal in-plane displacements ($v_1 = 0$), while we leave the transverse displacement undetermined, and instead impose zero slope, $\partial w/\partial X_1 = 0$. The interaction parameter is given by $\mathcal{I} = 12\mu\mathcal{U}_{u_1u_2}\mathcal{L}^2_{x_1x_2}/\mathcal{A}K$.

0.3.3 Problem setup – symmetric, fixed U_B

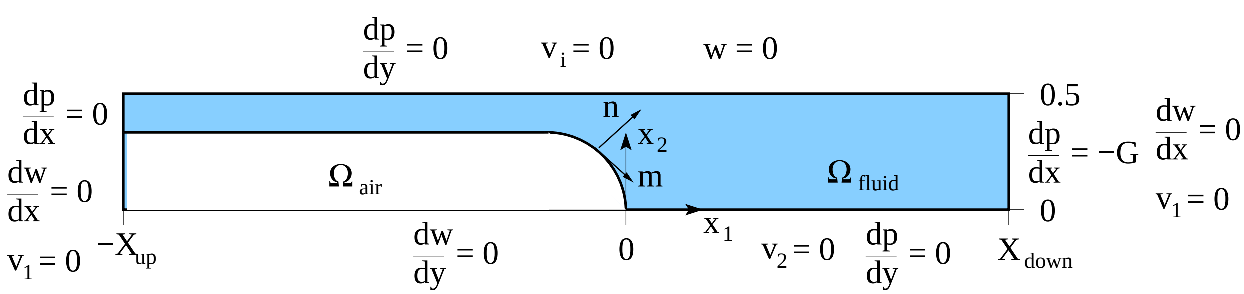

Figure 3: A schematic diagram of a symmetric, semi-infinite bubble propagating into an elasto-rigid channel. Boundary conditions as shown, where p is the fluid pressure, w the transverse displacement of the elastic sheet, and v_i the in-plane displacements of the sheet.

In order to trace only the symmetric solutions of the system, we enforce symmetry of the system by only modelling half of the domain, as shown schematically in Fig. 3. The boundary conditions are very similar to the full system – only the symmetry boundary requires special attention. At this boundary we impose zero normal flow, $\partial p/\partial X_2 = 0$ and leave the transverse displacement undetermined, while we impose zero slope, $\partial w/\partial X_1 = 0$, and zero normal in-plane displacements, $v_2 = 0$. In addition, at the bubble tip we enforce normal contact of the bubble interface with the symmetry boundary by setting the X_1-component of the tangent at that point to zero.

0.3.4 Problem setup – full, variable U_B

Instead of prescribing the tip velocity to a fixed value, we can determine it as part of the solution process and prescribe the volume flux into the bubble. The boundary conditions are identical to those shown in Fig. 2, while the non-dimensionalisation is based on the volumetric flow rate $\dot{V}$, as detailed in the description of the lab frame setup. Again, we hold the streamwise position of the tip of the air bubble at a prescribed position, $x_{\text{prescribed}} = 0$, which is used as a constraint to determine the unknown pressure in the air bubble, p_B. Far ahead of the bubble we apply the streamwise pressure gradient $\partial p/\partial X_1 = -G$, which is unknown *a priori* and is now determined such that the area and not the flux (since U_B is no longer 1) ahead of the bubble corresponds to the prescribed value, A_∞. The additional equation required to determine U_B is that the volumetric flow into the bubble corresponds to the prescribed value of 1 (since all quantities are non-dimensionalised on $\dot{V}$).

0.4 FEM formulation

When deriving the FEM formulation of our problem, we consider the most general case of the moving frame configuration with thin film corrections, because it can be easily simplified to the other cases considered herein. For clarity we drop the moving frame notation and work in the usual notation (x_1, x_2, x_3, t) instead. Hence, the residual equation for the unknown fluid pressure is given by

$$r_l^{[p]} = \iint_{\Omega_{\text{fluid}}} \left(\frac{\partial b}{\partial t} - \frac{\partial}{\partial x_i} \left[b^3 \frac{\partial p}{\partial x_i} \right] - U_{B,i} \frac{\partial b}{\partial x_i} \right) \psi_l \, \mathrm{d}x_1 \mathrm{d}x_2. \tag{74}$$

We integrate the second term by parts to yield

$$r_l^{[p]} \;=\; \iint_{\Omega_{\text{fluid}}} \left[\frac{\partial b}{\partial t}\, \psi_l + b^3 \frac{\partial p}{\partial x_i} \, \frac{\partial \psi_l}{\partial x_i} - U_{B,i} \frac{\partial b}{\partial x_i}\, \psi_l \right] \mathrm{d}x_1 \mathrm{d}x_2 \;-\; \oint_{\partial\Omega_{\text{fluid}}} b^3 \frac{\partial p}{\partial x_i} \; n_i \psi_l \; \mathrm{d}S. \tag{75}$$

The line integral is essentially the normal flux through the thickness of the Hele-Shaw cell, along a line in the (x_1, x_2)-plane, where the integrand is given by $-b\bar{u}_i\, n_i - bU_{B,i}\, n_i$. At the air-liquid interface, where the kinematic boundary condition applies, the integrand becomes

$$-b \frac{\partial R_i}{\partial t}\, n_i - bU_{B,i}\, n_i + b\, f_1(Ca) \frac{\partial R_i}{\partial t}\, n_i + b^3\, f_1^3(Ca) \frac{\partial p}{\partial x_i}\, n_i + b\, f_1(Ca) U_{B,i}\, n_i \quad \text{at } \partial\Omega_{\text{air}}, \tag{76}$$

where the pressure gradient is the one in the films. We discretise the biharmonic operator in (31) using a standard mixed formulation, based on independent interpolations for the membrane displacement w, its Laplacian $l^{[w]} = \nabla^2 w$, and the in-plane displacements v_i: $w = \sum_l W_l \psi_l$, $l^{[w]} = \sum_l L_l^{[w]} \psi_l$ and $v_i = \sum_l V_{il} \psi_l$. The weak form of (31) yields the residual

$$r_l^{[w]} = -\int_\Omega \frac{\partial^2 l^{[w]}}{\partial x_k^2}\, \psi_l \, \mathrm{d}x_1 \mathrm{d}x_2 + \int_\Omega \eta \frac{\partial}{\partial x_j} \left(\sigma_{ij}\, \frac{\partial w}{\partial x_i} \right) \psi_l \, \mathrm{d}x_1 \mathrm{d}x_2 + \int_\Omega P\, \psi_l \, \mathrm{d}x_1 \mathrm{d}x_2 = 0, \tag{77}$$

where $\Omega = \Omega_{\text{fluid}} \cup \Omega_{\text{air}}$. We integrate the first and second terms by parts to yield

$$\int_{\Omega} \frac{\partial^2 l^{[w]}}{\partial x_k^2}\, \psi_l \, \mathrm{d}x_1 \mathrm{d}x_2 = -\int_{\Omega} \frac{\partial l^{[w]}}{\partial x_k}\, \frac{\partial \psi_l}{\partial x_k} \, \mathrm{d}x_1 \mathrm{d}x_2 + \oint_{\partial\Omega} \left(\frac{\partial l^{[w]}}{\partial x_k}\, n_k \right) \psi_l \, \mathrm{d}S, \tag{78}$$

and

$$\int_{\Omega} \eta \frac{\partial}{\partial x_j} \left(\sigma_{ij}\, \frac{\partial w}{\partial x_i} \right) \psi_l \, \mathrm{d}x_1 \mathrm{d}x_2 = \\ - \int_{\Omega} \eta \sigma_{ij} \frac{\partial w}{\partial x_i} \frac{\partial \psi_l}{\partial x_j} \, \mathrm{d}x_1 \mathrm{d}x_2 + \oint_{\partial\Omega} \left(\eta \sigma_{ij} \frac{\partial w}{\partial x_i}\, n_j \right) \; \psi_l \, \mathrm{d}S, \tag{79}$$

respectively. Substituting (78) and (79) into (77) yields the combined residual

$$r_l^{[w]} = \int_{\Omega} \left(\frac{\partial l^{[w]}}{\partial x_k}\, \frac{\partial \psi_l}{\partial x_k} - \eta \sigma_{ij} \frac{\partial w}{\partial x_i} \frac{\partial \psi_l}{\partial x_j} + P\, \psi_l \right) \mathrm{d}x_1 \mathrm{d}x_2 \\ + \oint_{\partial\Omega} \left(\frac{\partial l^{[w]}}{\partial x_k}\, n_k + \eta \sigma_{ij} \frac{\partial w}{\partial x_i}\, n_j \right) \; \psi_l \, \mathrm{d}S = 0, \tag{80}$$

which we treat as the equation for the unknown nodal values of the transverse displacement, W_l. We determine the Laplacian of w from the projection equation

$$r_l^{[l^{[w]}]} = \int_{\Omega} \left(-\frac{\partial^2 w}{\partial x_k^2} + l^{[w]} \right) \psi_l \, \mathrm{d}x_1 \mathrm{d}x_2 = 0, \tag{81}$$

where we integrate the Laplacian by parts, similarly to (78), which yields

$$r_l^{[l^{[w]}]} = \int_{\Omega} \left(\frac{\partial w}{\partial x_k} \frac{\partial \psi_l}{\partial x_k} + l^{[w]}\, \psi_l \right) \, \mathrm{d}x_1 \mathrm{d}x_2 - \oint_{\partial\Omega} \left(\frac{\partial w}{\partial x_k}\, n_k \right) \, \psi_l \, \mathrm{d}S = 0. \tag{82}$$

The weak form of (32) yields the residual

$$r_{il}^{[v]} = \int_{\Omega} \left(-\frac{\partial \sigma_{ij}}{\partial x_j} + t_i \right) \, \psi_l \, \mathrm{d}x_1 \mathrm{d}x_2 = 0. \tag{83}$$

We integrate the first term by parts to give

$$\int_{\Omega} \frac{\partial \sigma_{ij}}{\partial x_j}\, \psi_l \, \mathrm{d}x_1 \mathrm{d}x_2 = -\int_{\Omega} \sigma_{ij} \frac{\partial \psi_l}{\partial x_j} \, \mathrm{d}x_1 \mathrm{d}x_2 + \oint_{\partial\Omega} \sigma_{ij}\, n_j\, \psi_l \, \mathrm{d}S. \tag{84}$$

Substituting these terms yields the residual equations

$$r_{il}^{[v]} = \int_{\Omega} \left(\sigma_{ij} \frac{\partial \psi_l}{\partial x_j} + t_i\, \psi_l \right) \, \mathrm{d}x_1 \mathrm{d}x_2 - \oint_{\partial\Omega} \sigma_{ij}\, n_j\, \psi_l \, \mathrm{d}S = 0, \tag{85}$$

which we treat as equations for the unknown nodal values of the in-plane displacements, V_{il}.

0.4.1 Lab frame

In the lab frame, the volume occupied by the bubble is computed from

$$V_{\text{bubble}} = \iint_{\Omega_{\text{fluid}}} (1 - f_1(Ca))\, b \, \mathrm{d}x_1 \mathrm{d}x_2. \tag{86}$$

0.4.2 Moving frame, fixed U_B

In case of a moving frame, we have two global unknowns in addition to the nodal unknowns $(p, w, l^{[w]}, v_1, v_2)$: the bubble pressure p_B and the pressure gradient far ahead of the bubble G. The residual equation for the unknown bubble pressure is given by

$$r^{[p_B]} = x_{\text{bubble tip}} - x_{\text{prescribed}}, \tag{87}$$

where we compute the bubble pressure such that the bubble tip remains fixed at the prescribed position $x_{\text{prescribed}}$.

The residual equation for the pressure gradient far ahead of the bubble is given by

$$r^{[G]} = \int_{\partial\Omega_{\text{a}}} b\, \bar{u}_1 \, \mathrm{d}x_2 - Q_\infty, \tag{88}$$

$$= \int_{\partial\Omega_{\text{a}}} \left(-b^3 \, \frac{\partial p}{\partial x_1} \; - \; U_{B,1} b \right) \, \mathrm{d}x_2 - Q_\infty, \tag{89}$$

where $\partial\Omega_{\text{a}}$ is the boundary far ahead of the bubble.

0.4.3 Moving frame, variable U_B

For a prescribed volumetric flow rate, U_B is no longer 1, so that the equation for the pressure gradient far ahead of the bubble has to be based on the area instead of the flux

$$r^{[G]} = \int_{\partial\Omega_{\text{a}}} b \, \mathrm{d}x_2 - A_\infty. \tag{90}$$

The equation for the unknown bubble tip velocity is given by

$$r^{[U_B]} = \int_{\partial\Omega_{\text{inflow}}} (1 - f_1(Ca))\, b\, U_B \, \mathrm{d}x_2 - 1, \tag{91}$$

where $\int_{\partial\Omega_{\text{inflow}}} (1 - f_1(Ca))\, b \, \mathrm{d}x_2$ represents the bubble cross section at the upstream end of the domain.

0.5 Results

The aim is to compare our numerical solutions with experimental results and we therefore use the following material parameters. The elastic sheet, which forms the top wall of the channel, has a thickness of $h = 0.34 \times 10^{-3}$ m, a Young's modulus of $E = 1.44 \times 10^{6}$ Pa and a Poisson ratio of $\nu = 0.5$. We apply a pre-stress to the membrane of $\sigma_{22}^{(0)*} = 40 \times 10^{3}$ Pa. The undeformed depth of the channel is $b_0 = 10^{-3}$ m and its width is $W_{\text{channel}} = 30 \times 10^{-3}$ m. The viscous fluid, which is displaced by the inviscid bubble, has a viscosity of $\mu = 0.099$ Pa s and a surface tension of $\gamma = 21 \times 10^{-3}$ N/m. We choose a bubble velocity of $U_B^* = 10^{-1}$ m/s.

These parameters result in an aspect ratio of $\mathcal{A} = 0.0333$, an interaction parameter of $\mathcal{I} = 1.53 \times 10^{4}$ and capillary number of $Ca = 0.47$. We prescribe the collapse of the channel far ahead of the bubble by setting $Q_\infty = A_i/A_0$. The computational domain covers $-10 \leq x_1 \leq 10$ and the bubble tip is kept at $x_{\text{prescribed}} = 0$.

Bibliography

Lev Davidovich Landau and Eugin M Lifshitz. *Course of Theoretical Physics Vol 7: Theory of Elasticity*. Pergamon Press, 1959.

Gunnar G Peng, Draga Pihler-Puzović, Anne Juel, Matthias Heil, and John R Lister. Displacement flows under elastic membranes. part 2. analysis of interfacial effects. *Journal of Fluid Mechanics*, 784:512–547, 2015.

DA Reinelt and PG Saffman. The penetration of a finger into a viscous fluid in a channel and tube. *SIAM Journal on Scientific and Statistical Computing*, 6(3):542–561, 1985.